Article

Not peer-reviewed version

Fracture Analysis and a Novel Relation Between the Quality of Interface and the Fracture Energy to Epoxy Composites Reinforced with Medium and High Ramie Woven Fabric Volume Fractions

Marcelo Machado *, Felipe Perissé Duarte Lopes, Noan Tonini Simonassi *, Eduardo Atem de Carvalho, Carlos Maurício Fontes Vieira, Sergio Neves Monteiro

Posted Date: 6 December 2024

doi: 10.20944/preprints202412.0627.v1

Keywords: Fracture Analysis; Natural Fibers; Biocomposite; Interface Quality; Fracture Energy

 doi:10.20944/preprints202412.0627.v1

Article

Fracture Analysis and a Novel Relation Between the Quality of Interface and the Fracture Energy to Epoxy Composites Reinforced with Medium and High Ramie Woven Fabric Volume Fractions

Marcelo Vitor Ferreira Machado [1,*], Felipe Perissé Duarte Lopes [2], Noan Tonini Simonassi [2,*], Eduardo Atem de Carvalho [2], Carlos Maurício Fontes Vieira [2] and Sergio Neves Monteiro [2,3]

[1] Mechanical Engineering Department, Fluminense Federal Institute (IFF) and Nucleus of Studies in Applied Thermomechanics, Campos dos Goytacazes, Rio de Janeiro, Brazil
[2] Materials Science Department, State University of Northern Rio de Janeiro (UENF), Advanced Materials Laboratory (LAMAV), Campos dos Goytacazes, Rio de Janeiro, Brazil
[3] Materials Science Program, Military Institute of Engineering, Rio de Janeiro, Rio de Janeiro, Brazil
* Correspondence: marcelo.machado@iff.edu.br (M.V.F.M.); noantoninisimonassi@gmail.com (N.T.S.)

Abstract: A literature review in the context of polymer composites reveals that the natural fibers have been widely used as reinforcement phase, at least, in the last two decades. In this development direction, the lignocellulosic fibers have been highlighted due to their environmental, thermomechanical and economic advantages to many industry sectors. This research aims to analyze experimentally the fracture of ramie woven fabric reinforced epoxy composite specimens subjected to Charpy test and based on specific theoretical knowledge, to state a novel relationship between the quality of interface and the fracture energy. To reach this objectives, the study is designed with three groups (40%, 50% and 60% of fiber volume fractions) of intact samples and three groups of C-UV aged specimens containing the same percentage of reinforcement. Afterwards, a fracture surface analysis is done to support the study about the samples fracture behavior and describe the referred relation introducing an interface quality variable. According to the results obtained, could be concluded that the relationship proposed is in congruence with the fracture surface characterizations made.

Keywords: fracture analysis; natural fibers; biocomposite; interface quality; fracture energy

1. Introduction

Specially in last two decades, the polymer composites reinforced with natural fibers have been widely studied due to their eco-friendly and sustainable characteristics, as well as, advantages like abundant sources and low acquisition cost make them even more attractive to elevate the competitiveness of some industries. Furthermore, the thermomechanical properties presented by the polymer composites reinforced with lignocellulosic fibers have been interesting to the automotive, energy, aerospace and civil construction sectors [1–14].

In conformity with (Rafiee, K. et al. [15]; Muniyasamy, S. and Dada [16]) a composite using at least one of the components (matrix or reinforcements) from natural source can be considered as a biocomposite. This class of alternative multiphase materials have had a crucial relevance in the process of energy transition, since they can reduce the equivalent $C0_2$ emissions during the life-cycle of some equipment of renewable energy sector by the replacing of traditional materials still used in them [17]. These substitutions can become the renewable industries even more sustainable and greener in the context of novel recycling process to the thermoset resins have been developed recently [18].

It is a well known fact that the adhesion level between fibers and polymer matrix has relevance in the mechanical performance and, consequently, in the failure behavior of laminates. The quality of the interface is even more critical in that context when natural fibers are used as reinforcement in the

 doi:10.20944/preprints202412.0627.v1

composition of this kind of heterogeneous materials due to the multiple physical and chemical characteristics of them. According to the aforementioned condition, this research suggest a relationship between the quality of interface and the fracture process to the ramie reinforced epoxy composite produced based on specific literature data, the Hamilton's principle and the experimental observations regarding to the Charpy tests.

Some question can be done here, for example: What is the influence of the interface quality in the development of intralaminar and/or interlaminar fracture in that biocomposite subjected to impact load? What are the fracture profiles differences observed when the fiber volume fraction is elevated from medium to high ones? And after the C-UV aging simulation, what happened with the fracture behavior of the laminate due to the impact loads?

The objective of this study is to bring answers to the above formulated questions making a fracture analysis of the manufactured laminate specimens containing medium and high ramie theoretical volume fractions and, of course, states a relation to describe how the interface quality is associated with the fracture behavior of the studied heterogeneous material.

Using inferential analyses to evaluate the statistical differences or not among the central values obtained to the absorbed energy, notch toughness and impact strength, this research develop a fracture analysis aiming to propose a relationship between the quality of interface and the fracture energy of the specimens subjected to the Charpy test. Finally, an appropriate and satisfactory expression is obtained from the analysis and can support a technological advance concerning the impact properties to the polymer biocomposites.

2. Materials and Methods

2.1. Production of Composite Plates

The first process was to determine the density of ramie fiber in the acquired woven fabric using four pycnometers based on ISO 4787 [20]. Ten measurements were made in each glass instrument and the mean obtained ($\rho = 1{,}495 \frac{g}{cm^3}$) is in congruence with literature values, for example, as the calculated in Uppal et al [21]. That result has been used to determine the number of ramie woven fabric plies to 40%, 50% and 60% of fiber theoretical volume fractions according to the mold volume, see Table 1.

Table 1. Number of ramie woven fabric plies to the fiber theoretical volume fractions used.

Test	40%	50%	60%
	Number of plies	Number of plies	Number of plies
Charpy	70	87	105

The exposure of ramie woven fabric plies in a stove during 24 hours at 60° were made to remove moisture from them. Afterwards, a blend of epoxy resin (DGEBA/TETA MD 130) and hardener (FD 129) were done manually during three minutes in a mass ratio of 1:0,13 and then, the fiber plies and the aforementioned mixture were compressed in a mold using 6000 kgf/cm² (corrected during 20 minutes). Finally, one day after that, the biocomposite plates were removed from mold.

Six plates were produced, three (40%, 50% and 60% of fiber theoretical volume fractions) to intact (non aged) specimens and three (the same medium and high fiber percentage) to condensation-ultraviolet (C-UV) aged specimens, as can be seen in the next section.

 doi:10.20944/preprints202412.0627.v1

2.2. Impact Tests

The Charpy impact tests have been performed according to standardization ISO 179-1using intact and C-UV aged specimens (Figure 1) in a Pantec manufacturer equipment (Figure 2). In summary, the experiments have been designed with the three groups (40%, 50%, 60%) of called intact specimens and the same number of groups to the aged ones.

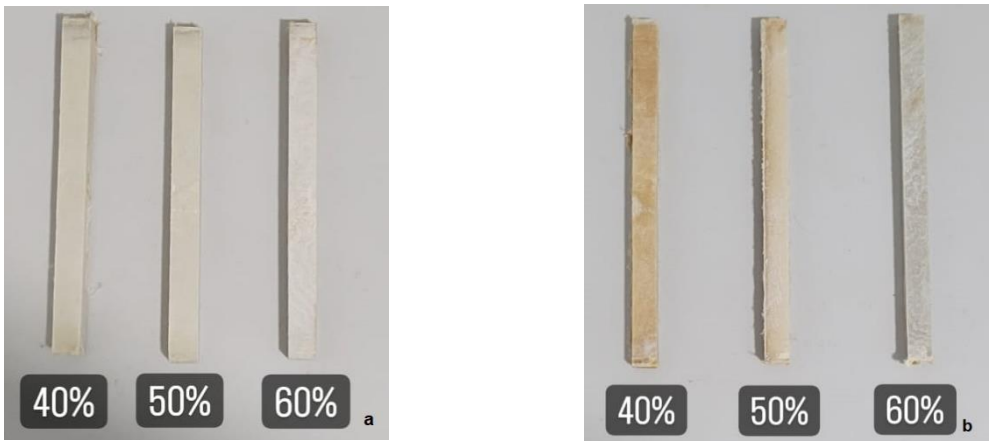

Figure 1. (1a) intact specimens and (1b) aged specimens used in Charpy tests [22].

Figure 2. Impact test equipment used in the experiments with the laminate specimens [22].

To the C-UV aging process were used an accelerated equipment from ADEXIM-COMEXIM manufacturer (Figure 3) according to ASTM-G53/154 [23]. The simulation conditions were set up based on ASTM 5208 and ADEXIM-COMEXIM correlation [25]. Regarding to this correlation, could be set up 504 hours of exposure at 70 °C in a cycle of 8 hours in the aging system and then, that accelerated process was equivalent to 9 months of real exposure, approximately [22].

 doi:10.20944/preprints202412.0627.v1

Figure 3. C-UV accelerated aging system from ADEXIM-COMEXIM manufacturer [22].

The descriptive statistics of experimental data and graphs were made using Origin 6.0 software and the inferential analysis has been performed in PAST 4.03 computational tool. It is relevant to mention that in the case of intact specimen experimental data, non-parametric tests (Kruskal-Wallis and Dunn) were used due to verified non-normality of the linear regression residuals. To the aged specimen data, one-way ANOVA and Tukey tests could be calculated [22].

Some specific fracture surface characterizations have been obtained using the Scanning Eletron Microscope (SEM) showed from the Figure 4. Firstly, the fracture surface of intact specimen number 2 of 40% group (which presented the lowest impact strength of all specimens tested) was analyzed at 45x, 120x, 300x and 700x magnification, in addition, the delaminated surface of specimen number 8 of 60% group (also with a low impact strength) has been observed at 20x, 36x, 100x, 300x magnification. These characterizations are relevant to the research because they reveal some specific differences between intralaminar fracture and the delamination mechanism according to the matrix-fiber adhesion quality, as shall be seen further.

Figure 4. Shimadzu SSX550 Scanning Eletron Microscope used to characterize the fracture surfaces.

 doi:10.20944/preprints202412.0627.v1

2.3. Considerations to the Quality of Interface and Fracture Energy Relationship

In the Charpy test, due to the impact of hammer on the marked region in the Figure 5, instant reactions on supports contribute to the bending of the specimen. Consequently, tensile stress is developed in the sample making the dynamical opening of the notch and successive crack propagation from its tip, as indicated on Figure 6.

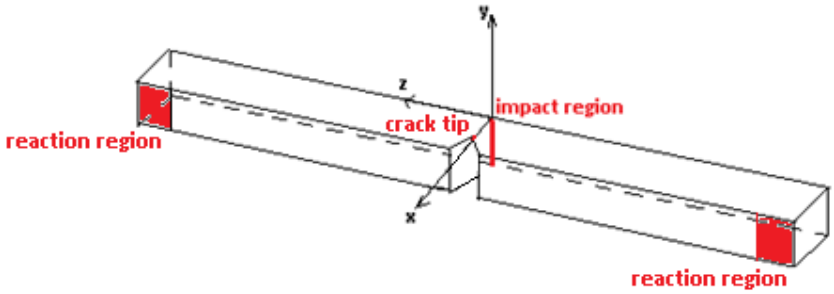

Figure 5. Sketch of Charpy test specimen with relevant regions highlighted.

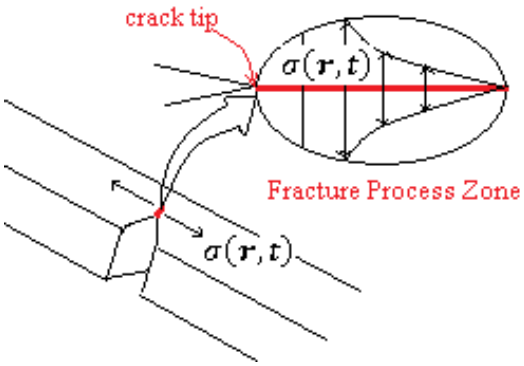

Figure 6. Tensile stress field developed from the impact load during the Charpy test.

As indicated in the Figure 6, this stress field is a function of the space and time, where $\mathbf{r} = \mathbf{r}(x,y,z)$ is the position vector of any point inside the fracture process zone [26–35]. The crack propagation occurs from the stress concentration initial point, the tip of the notch. This initial position is $\mathbf{r}_0$ and according to the geometric path done by the crack tip during the failure process, the final position vector can be determined.

Based on the Hamilton's principle can be written that: among all possible paths to the crack tip, it will develop that path in which the action is stationary, in other words, as the crack has its evolution during a given time interval ($\Delta t = t_2 - t_1$), the geometric path developed by the crack tip must be that with the lowest consumed energy to the fracture process.

The lowest absorbed energy by a specimen during a fracture process at any point and instant has an upper limit that is the necessary energy to maintain the continuous deformation in the material, which can be written as:

$$E(\boldsymbol{r},t) = \int(\int \sigma(\boldsymbol{r},t)\boldsymbol{n}dA).\boldsymbol{dr} \qquad (1)$$

Where dA is the oriented infinitesimal area upon which the stress field acts and **dr** is the infinitesimal displacement vector of the considered material point, see Figure 7.

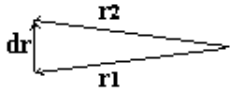

Figure 7. The infinitesimal displacement vector during a continuous deformation.

 doi:10.20944/preprints202412.0627.v1

Obviously, the equation (1) is based on continuum hypothesis and will present limitations concerning the presence micro cracks, lack of adhesion in the matrix-fiber interfaces regions, i. e., any kind of discontinuity in the laminate. Another question is that $\sigma(\boldsymbol{r},t)$ will present jumps in phase transition regions, then, the integral in (1) must be done step by step in domains where the properties have a smooth continuity.

Considering the presence of all possible kind of the discontinuities in material and that the fracture energy is lower than $E(\boldsymbol{r},t)$, this study assumes that real absorbed energy in the fracture process can be written as a general inequality below:

$$W_{intra} + W_{inter} < E(\boldsymbol{r},t) \quad (2)$$

where W_{intra} and W_{inter} are the works of the intralaminar and interlaminar fractures in the laminate.

According to the specific literature, the fiber reinforced polymer composites present, in general, a quasi-brittle fracture behavior with multiple mechanisms of failure. Intralaminar and interlaminar failures, as well as, combinations between them must be accounted in fracture process zone to improve the predictions about the failure phenomena in laminates [36–47].

Aiming to describe a relation between the absorbed energy in the fracture processes of the manufactured biocomposites with the quality of the matrix-fiber interface, this research proposes the definition of a variable such as:

$$0 \leq \xi \leq 1 \quad (3)$$

where the value 0 refers to a very low quality (absent of adhesion between continuous and dispersed phases) and 1 represents a very high quality (matrix-fiber strongest adhesion) to the interface.

In this context, depends on the results analysis of the fracture processes with the samples used in the research, the quality of interface variable will be introduced in the general inequality (2).

3. Results and Discussion

3.1. Results to the Charpy Test in Intact Specimens

To the intact specimens with 40%, 50% and 60% of theoretical volume fractions, the means of energy(J), notch toughness (J/m) and impact strength (J/m²) can be seen from Table 2 (see Appendix A to each singular measurement). The specific trend analysis relating the impact strength and the theoretical volume fractions is shown from Figure 8.

Table 2. Means and standard deviation of Charpy tests using intact specimens with 40%, 50% and 60% of fiber theoretical volume fractions.

%Vol$_{fiber}$	Energy (J)	Notch Toughness (J/m)	Impact Strength (kJ/m²)
40%	1,28 ± 0,35	139,91 ± 37,67	21,83 ± 6,08
50%	1,48 ± 0,36	158,53 ± 36,10	24,45 ± 4,59
60%	3,86 ± 1,87	414,09 ± 200,24	49,67 ± 25,44

 doi:10.20944/preprints202412.0627.v1

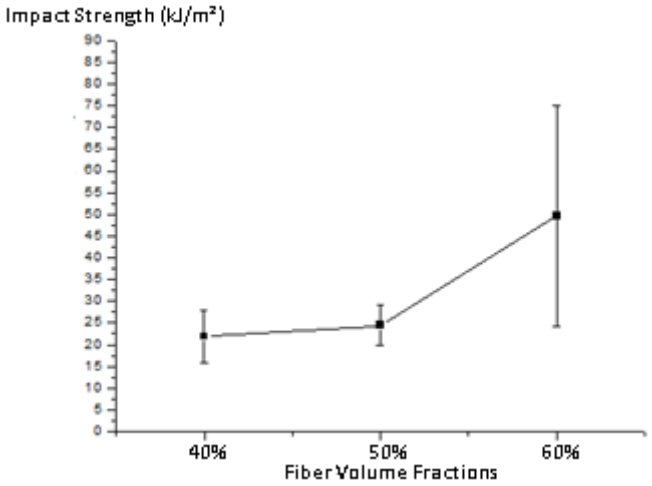

Figure 8. Impact strength X Fiber volume fractions to the means of intact specimens.

Conforming to Table 2 and Figure 8 can be noticed a disproportionate standard deviation to the 60% theoretical volume fraction specimens. It is believed that this large statistical measurement can be related to the small amount of epoxy resin combined to its poor distribution in the composite plate manufactured, since it was a hard manual task due to more than one hundred ramie woven fabric layers used in that. These two conditions lead to 60% specimens with a substantial variation regarding to the quality of interface adhesion between matrix and fiber, resulting in a large variance observed and, as an author's suggestion, more samples must be used to this high volume fraction (60%) in future studies.

The idea discussed in the last paragraph is illustrated in the Figure 9 below, where can be perceived some different fracture surface profiles. For example, the specimen number 7 has a classical brittle fracture, with the smallest fracture surface observed and consequently, it has absorbed a small amount of impact energy and, in a practical evaluation, this specimen had only intralaminar fractures. To other specimens in the Figure 9, can be observed delamination regions on fracture surfaces. This kind of interlaminar failure increases the crack tip path, what means higher amount of impact absorbed energy.

Figure 9. Some fracture surface profiles of intact specimens with 60% of theoretical volume fraction.

An inferential analysis to the impact strengths from Table 2 needed to be developed using Kruskal-Wallis and Dunn tests because the linear regression residuals did not present a normal distribution in conformity with Shapiro-Wilk test. According to those non-parametric analyses, only the central values calculated to the intact specimens with 40% and 50% of fiber theoretical volume

 doi:10.20944/preprints202412.0627.v1

fractions can be considered statistically equals (marked in light blue, Table 3). The means obtained to 40% and 60%, 50% and 60% are different considering 5% of significance level.

Table 3. Results of Dunn post hoc test to impact strength experimental data of intact specimens.

	40%	50%	60%
40%		0,2423	0,0002812
50%	0,2423		0,0146
60%	0,0002812	0,0146	

3.2. Results to the Charpy Test in Aged Specimens

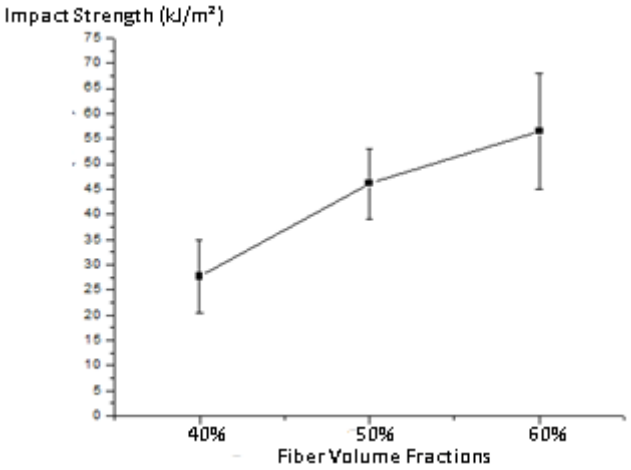

Figure 10. Impact strength X Fiber volume fractions to the means of C-UV aged specimens.

From Table 4 can be seen means and standard deviations to the results of impact tests with the three groups of C-UV aged specimens. The first noTable information from these data are the higher means of energy, notch toughness and impact strength than means to intact specimens. This fact shows that impact properties did not suffer degradation by the C-UV aging proposed in this study, in contrast with it, the properties were improved, probably due to a post cure effect over the biocomposite aged plates.

Table 4. Means and standard deviation of Charpy tests using C-UV aged specimens with 40%, 50% and 60% of fiber theoretical volume fractions.

$\%Vol_{fiber}$	Energy (J)	Notch Toughness (J/m)	Impact Strength (kJ/m^2)
40%	2,31 ± 0,77	231,11 ± 76,60	27,62 ± 7,25
50%	3,54 ± 0,61	354,40 ± 61,12	46,11 ± 6,59
60%	4,55 ± 1,18	455,00 ± 118,22	56,47 ± 11,55

The trend of impact strength elevation according to the growing fiber volume fractions is repeated in this case. This behavior has already been observed to intact specimens, but now, the C-UV aged specimens have shown a coefficient of variation lower to each fiber volume fraction

 doi:10.20944/preprints202412.0627.v1

considered than in the case of intact specimens. For while, can be only said that there is a correlation between aging process and the growing of impact strength means, as well as, with the decrease in the coefficients of variation.

After the Shapiro-Wilk test revealed a normal distribution to the linear regression residuals, an ANOVA and a Tukey test were done and presented a statistical equality to the aged specimens means with 50% and 60% of fiber theoretical volume fractions considering 5% of significance level.

Table 5. Tukey test results to the comparison among aged specimens means.

	40%	50%	60%
40%		0,0004976	1,095E-06
50%	6,27		0,05142
60%	9,783	3,513	

3.3. The Quality of Interface and Fracture Energy Relantionship

To insert the variable that represent the quality of interface in the general energy inequality (2) it is necessary to analyze the fracture profiles of the samples used to investigate how the adhesion between matrix and fiber affects the development of intralaminar and/or interlaminar fractures. Randomly, could be taken pictures of some specimens of all groups used in the experiment and the fracture profiles have been analyzed.

As can be seen from the Figure 11, the majority of fracture profiles have fractured with significant bumpy surface, alternating small and short delaminations with intralaminar ruptures. A fracture surface characterization of some intact specimens tested support the analysis of this study. The SEM has been used to observe the fracture surface of the intact specimen number 2 with 40% of fiber theoretical volume fraction, which had the smallest impact strength among all experimented samples.

Figure 11. Some fracture profiles of intact specimens. 11A) 40%, 11B) 50% and 11C) 60% fiber theoretical volume fraction.

From the Figure 12 below, the yellow circled regions show ruptured fibers and red circled regions present some flat and smooth surfaces, what indicate that the crack tip taken a shorter path in an intralaminar fracture due to high quality of adhesion between continuous and dispersed phases for the above mentioned specimen. This kind of straight fracture surface and brittle was not exclusive to the intact 40% group, as can be seen in the top of Figure 12C.

Additionally, a delaminated surface also of an intact specimen with small impact strength were characterized and can be seen from Figure 13. In this case, the surface observation reveals a weak

 doi:10.20944/preprints202412.0627.v1

adhesion between matrix and fibers, because the poor distribution of epoxy resin (white particulate material) over the ramie woven fabric (in gray). This fact shows that the crack tip propagated through of an interlaminar region and then, the separation of composite layers happened.

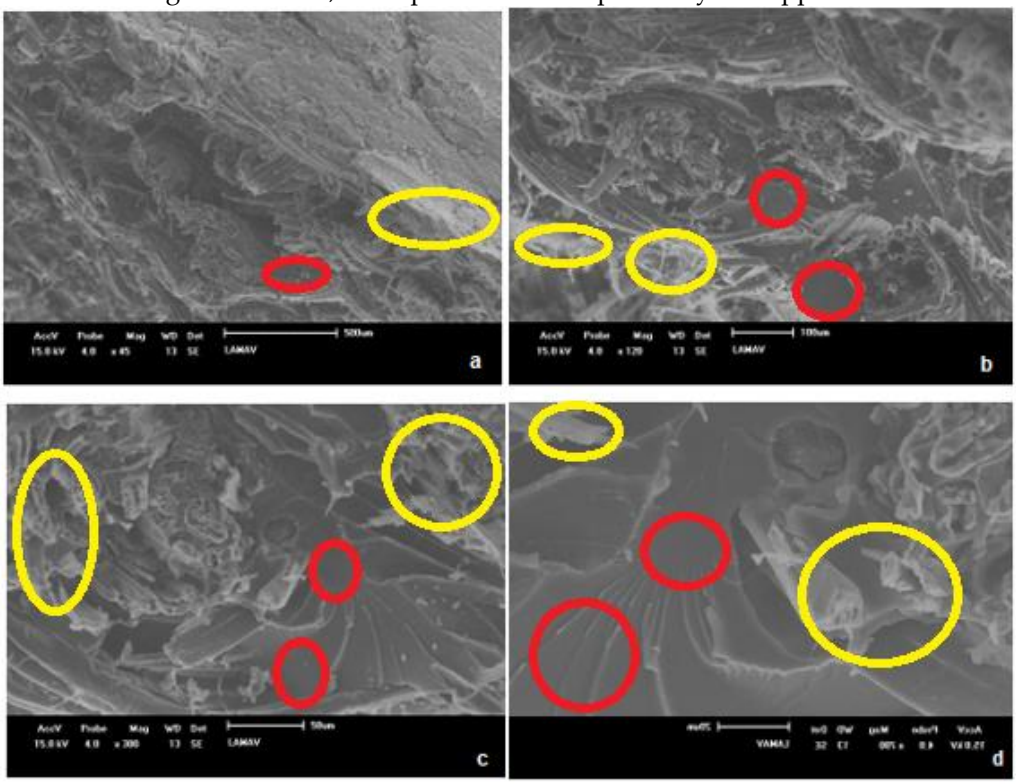

Figure 12. Fracture surface characterizationof the specimen with smallest impact strength. With 45x (12a), 120x (12b), 300x (12c) and 700x of magnification (12d).

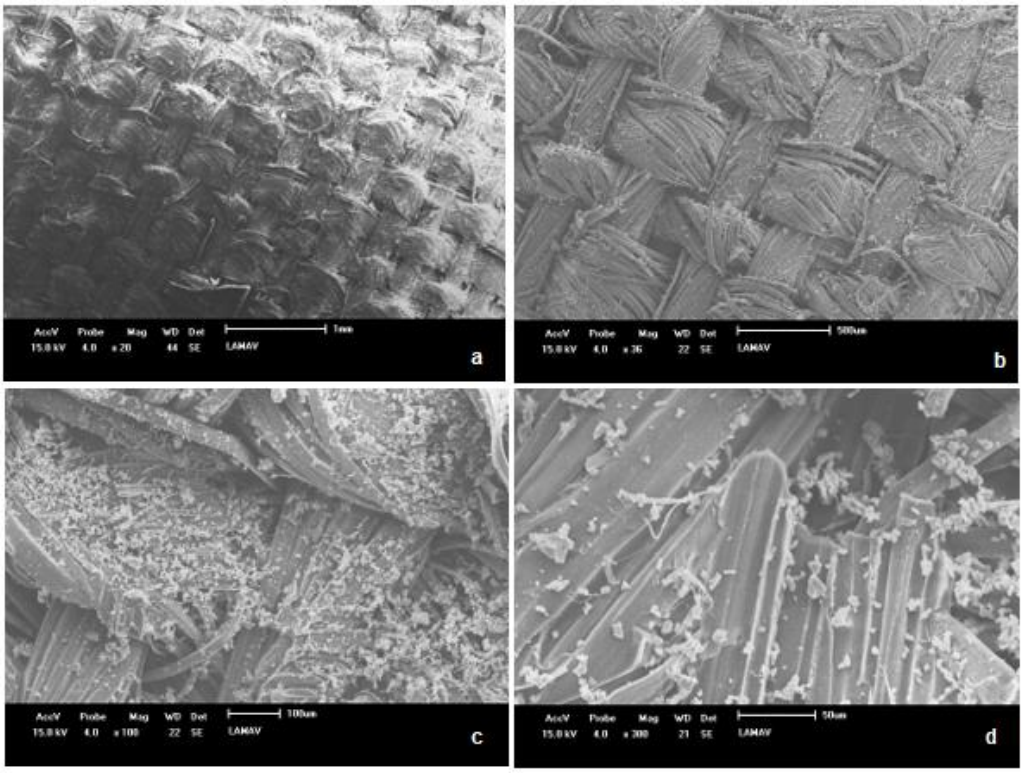

Figure 13. Delaminated fracture surface of an intact specimen with weak adhesion to the interface. With 20x (13a), 36x (13b), 100x (13c) and 300x of magnification (13d).

 doi:10.20944/preprints202412.0627.v1

In general, to the C-UV aged samples, the fracture behavior of the ramie reinforced epoxy composite with medium and high percentage of fibers were the same observed to the intact ones. Most part of specimens presented a fracture surface with successive interaction between intralaminar and interlaminar failures, but in details, specimens with straight fracture surfaces and and a great delamination with low absorbed energy were not seen. This fact corroborates with a higher concentration to the values of ξ about the variable mean and, then, a moderate quality of interface has been achieved in more cases to the aged specimens, what can also be seen through the higher impact strength means than intact samples and lower standard deviations obtained to the C-UV aged groups in relation to the intact ones.

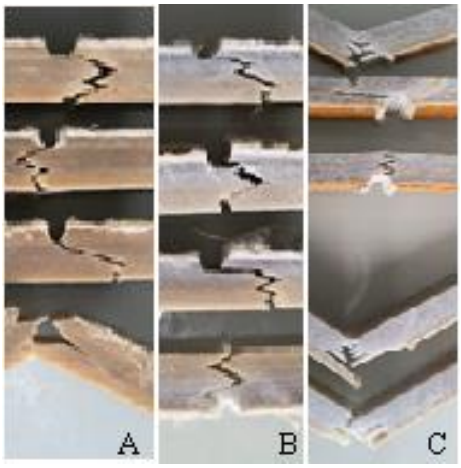

Figure 14. Some fracture profiles of C-UV aged specimens. 14A) 40%, 14B) 50% and 14C) 60% fiber theoretical volume fraction.

As a result of the observations done through the Charpy tests with the ramie reinforced epoxy composites produced samples, the relationship (4) can be written to describe how the quality of interface is associated with each kind of fracture and how the general quasi-brittle behavior, due to presence of multiple discontinuities in the material, limits the value of absorbed energy in comparison with a continuum model.

$$\xi W_{intra} + (1 - \xi) W_{inter} < E(\boldsymbol{r}, t) \quad (4)$$

From the inequality (4) is trivial to realize that to the highest quality of interface (ξ = 1) and to lowest one (ξ = 0) the samples do not present an interaction between intra and interlaminar fractures and then, there are not an efficient absorption of energy during impact loading over the considered biocomposites.

4. Conclusions

In congruence with the discussion make in the last section, can be concluded that the quality of interface is directly related to the development of intralaminar, as well as, to the process of interlaminar failures. In this sense, could be seen that a moderate quality to the interface between matrix and fibers is the best condition to the epoxy composite reinforced with ramie woven fabric regarding to the impact strength.

Concerning the topography of the fracture surfaces, were not observed many macroscopic differences between the failure processes of intact and C-UV aged samples, in general. To the first groups above mentioned, could be noted some specimens with very straight and smooth surfaces (which indicates a brittle fracture due to very strong adhesion in the interfaces) and also very delaminated fracture profiles, what represents very weak adhesion in the matrix-fibers interfaces. Nevertheless, in general, the majority of fracture surfaces of the intact specimens shown a similar profile with the C-UV aged samples, which, in turn, did not present very strong or very weak adhesions between continuous and dispersed phases.

 doi:10.20944/preprints202412.0627.v1

Another detail is that the means of C-UV aged samples impact strength were higher than to the intact ones considering the same fibers percentage and that the standard deviation calculated in each case were lower than the respective non aged specimens with the same fiber volume fractions. This fact reveals a higher concentration of the values related to the variable ξ around the defined mean value (0.5) to the C-UV aged samples than to the intact ones.

In summary, the fracture analysis done to the epoxy composite reinforced with ramie woven fabric using medium and high fiber percentage presented that a moderate interface quality is a desirable condition to the material strength when subjected to the impact load. This fact and the influence of the interface quality in the intralamnar and interlaminar fractures have been satisfactorily descripted from the novel relationship (inequality 4). These results can contribute to improvements regarding to strength of this eco-friendly laminate when in applications that exposure it to high strain rate. Hence, this research supports the insertion of a lignocellulosic fiber reinforced polymer composite in the industry sectors and this technological development can bring a higher sustainability and competitiveness to their process.

References

1. PARVATHANENI et al. Prediction of impact behaviour for natural fiber-reinforced composites using the finite element method. Composites and Advanced Materials, v. 31, 2022.
2. XU, B. et al. Effect of moisture in flax fiber on viscoelastic properties of the manufactured flax fiber reinforced polymer by fractional-order viscoelastic model. Materials Today Communications, v. 40, 2024.
3. SYDUZZAMAN et al. Natural Fiber Reinforced Polymer Composites for Ballistic Protection: Design, Performance, and Challenges. Results in Materials, 2024.
4. SONI, A. et al. An overview of recent trends and future prospects of sustainable natural fiber-reinforced polymeric composites for tribological applications. Industrial Crops and Products, v. 222, 2024.
5. KAREEM, A. et al. Influence of the stacking on mechanical and physical properties of jute/banana natural fiber reinforced polymer matrix composite. Materials Today Proceedings, 2023.
6. SINGH, M. K. et al. A comprehensive review of various factors for application feasibility of natural fiber-reinforced polymer composites. Results in Materials, v. 17, 2023.
7. KOPPULA , S. B. et al. Investigation into the mechanical characteristics of natural fiber-reinforced polymer composites: Effects of flax and e-glass reinforcement and stacking configuration. Materials Today Proceedings, 2023.
8. SEID, A. M.; ADIMASS, S. A. Review on the impact behavior of natural fiber epoxy based composites. Heliyon, v. 10, n. 20, 2024.
9. VISHWASH, B.; SHIVAKUMAR, N.D.; SACHIDANANDA., K.B. Analytical investigation of green composite lamina utilizing natural fiber to strengthen PLA. Hybrid Advances, 2024.
10. KHAN, F. et al. Advances of Natural Fibers Composites in Diverse Engineering Applications – A Review. Applications in Engineering Science, v. 18, 2024.
11. KUMAR, K. D. et al. Study the effect of fracture toughness on hybrid composite for automotive application. Materials Today Proceedings, v. 92, 2023.
12. MANSOR, M.R; NURFAIZEY, A.H.; TAMALDIN, N.; NORDIN, M.N.A. Natural fiber polymer composites: Utilization in aerospace engineering. In Woodhead Publishing Series in Composites Science and Engineering. Biomass, Biopolymer-Based Materials, and Bioenergy. Woodhead Publishing. Cambridge. 2019..
13. TULI, N. T.; KHATUN, S.; RASHID, A. B. Unlocking the future of precision manufacturing: A comprehensive exploration of 3D printing with fiber-reinforced composites in aerospace, automotive, medical, and consumer industries. Heliyon, 2024.
14. SANTOS, C. M. et al. A Bibliometric Review on Applications of Lignocellulosic Fibers in Polymeric and Hybrid Composites: Trends and Perspectives. Heliyon, v. 10, 2024.
15. RAFIEE, K. et al. Biodegradable green composites: It's never too late to mend. Current Opinion in Green and Sustainable Chemistry, v. 30, p. 100482–100482, 1 ago. 2021.
16. MUNIYASAMY, S; DADA, O. 2021. Recycling of plastics and composites materials and degradation technologies for bioplastics and biocomposites. Waste Management in the Fashion and Textile Industries: The Textile Institute Book Series.
17. EL KINANI, K. et al. Interdisciplinary analysis of wind energy - a focus on France. Sustainable Energy Technologies and Assessments, v. 55, p. 102944, 1 fev. 2023.
18. AHRENS, A. et al. Catalytic disconnection of C–O bonds in epoxy resins and composites. Nature, p. 1–8, 26 abr. 2023.

 doi:10.20944/preprints202412.0627.v1

19. UPPAL, N. et al. Cellulosic fibres-based epoxy composites: From bioresources to a circular economy. Industrial Crops and Products. Aug;182: 114895. Epub, 2022.
20. ISO 4787 – Laboratory Glass and Plastic Ware – Volumetric Instruments – Methods for testing of capacity and use. 2021.
21. ISO 179-1 – Plastic Determination of Charpy Impact Properties, part 1: Non-instrumented Impact Test. 2010.
22. MACHADO, M. V. F. et al. Ensaios de Impacto em Compósitos Epóxi com Média e Alta Frações Volumétricas Teóricas de Tecido de Rami e uma Análise de Fraturas à Luz do Princípio de Hamilton. ABM Proceedings, p. 321–332, 2024.
23. ASTM-G53/154 – Standard Practice for Operating Fluorescent Light Apparatus for UV Exposure of Nonmetallic Materials. 2017.
24. ASTM D 5208 - Standard Practice for Fluorescent Ultraviolet (UV) Exposure of Photodegradable Plastics. 2022.
25. ADEXIM-COMEXIM – Correlação Entre o Tempo Real de Intemperismo e a Ação do Sistema C-UV com Base na ASTM-G53/154. 2000.
26. WU, X. et al. Fracture process zone and fracture energy of heterogeneous soft materials. Journal of the Mechanics and Physics of Solids, p. 105997, 2024.
27. HOSSEIN IZADI, S. M.; FAKOOR, M.; MIRZAVAND, B. A novel mixed mode fracture criterion for functionally graded materials considering fracture process zone. Theoretical and Applied Fracture Mechanics, v. 134, 2024.
28. POP, I. O. et al. A new approach for fracture process zone evaluation. Theoretical and Applied Fracture Mechanics, v. 132, 2024.
29. OSHIMA, S. et al. Mesoscale mechanism of damage in fracture process zone of CFRP laminates simulated with triaxial stress state-dependent constitutive equation of matrix resin. Composites Science and Technology, v. 257, 2024.
30. MAGHAMI, A. et al. Bulk and fracture process zone contribution to the rate-dependent adhesion amplification in viscoelastic broad-band materials. Journal of the Mechanics and Physics of Solids, v. 193, 2024.
31. CHU, P. et al. Anisotropic fracture behavior and corresponding fracture process zone of laminated shale through three-point bending tests. Journal of Rock Mechanics and Geotechnical Engineering, 2024.
32. NIE, Y.; LI, D.; LUO, Q. A multiscale nonlinear fracture model for staggered composites to reveal the toughening effect of process zone. Composites Science and Technology, v. 241, 2023.
33. XU, X.; TAKEDA, S.; WISNOM, M. R. Investigation of fracture process zone development in quasi-isotropic carbon/epoxy laminates using in situ and ex situ X-ray Computed Tomography. Composites. Part A, Applied science and manufacturing, v. 166, 2023.
34. LIU, X.; ZHANG, H.; LUO, S. Size effect model of nominal tensile strength with competing mechanisms between maximum defect and fracture process zone (CDF model) for quasi-brittle materials. Construction and Building Materials, v. 399, p. 132538–132538, 23 jul. 2023.
35. SCOTT, D. A. et al. Fracture process zone characterizations of multi-scale fiber reinforced cementitious composites. Construction and Building Materials, v. 408, p. 133713–133713, 14 out. 2023.
36. SU, H.; WANG, L.; CHEN, B. A phase-field framework for modeling multiple cohesive fracture behaviors in laminated composite materials. Composite Structures, v. 347, 2024.
37. QU, Z.; ZHAO, C.; AN, L. A micromechanics perspective on the intralaminar and interlaminar damage mechanisms of composite laminates considering ply orientation and loading condition. Composite Structures, v. 347, 2024.
38. FERREIRA, L. M.; COELHO, C. A. C. P.; REIS, P. N. B. Numerical predictions of intralaminar and interlaminar damage in thin composite shells subjected to impact loads. Thin-Walled Structures, v. 192, 2023.
39. AO, W. et al. Finite element method of a progressive intralaminar and interlaminar damage model for woven fibre laminated composites under low velocity impact. Materials & Design, v. 223, 2022.
40. HE, R. et al. Dynamic tensile intralaminar fracture and continuum damage evolution of 2D woven composite laminates at high loading rate. Theoretical and Applied Fracture Mechanics, p. 104731–104731, 1 out. 2024.
41. HU, P. et al. An experimental study on the influence of intralaminar damage on interlaminar delamination properties of laminated composites. Composites Part A: Applied Science and Manufacturing, v. 131, 2020.
42. RUSSO, A.; PALUMBO, C.; RICCIO, A. The role of intralaminar damages on the delamination evolution in laminated composite structures. Heliyon, v. 9, n. 4, 2023.
43. TAN, W. et al. The role of interfacial properties on the intralaminar and interlaminar damage behaviour of unidirectional composite laminates: Experimental characterization and multiscale modelling. v. 138, p. 206–221, 2018.

 doi:10.20944/preprints202412.0627.v1

44. ESPADAS-ESCALANTE, J. J.; VAN DIJK, N. P.; ISAKSSON, P. The effect of free-edges and layer shifting on intralaminar and interlaminar stresses in woven composites. Composite Structures, v. 185, p. 212–220, 2018.
45. NAYA, F.; PAPPAS, G.; BOTSIS, J. Micromechanical study on the origin of fiber bridging under interlaminar and intralaminar mode I failure. Composite Structures, v. 210, p. 877–891, 2019.
46. DE MOURA, M. F. S. F. et al. Interlaminar and intralaminar fracture characterization of composites under mode I loading. Composite Structures, v. 92, n. 1, p. 144–149, 2010.
47. FISHER, J.; CZABAJ, M. W. A new test for characterization of interlaminar tensile strength of tape-laminate composites. Composites Part A Applied Science and Manufacturing, v. 176, p. 107868–107868, 26 out. 2023.